Future reef decalcification under a business-as-usual CO_2 emission scenario

Sophie G. Dove[a,b,c,1], David I. Kline[a,b,2], Olga Pantos[a,b], Florent E. Angly[d], Gene W. Tyson[d,e], and Ove Hoegh-Guldberg[a,b,c]

[a]Global Change Institute, [b]School of Biological Sciences, [c]Australian Research Council Centre for Excellence in Coral Reef Studies, [d]Australian Centre for Ecogenomics, and [e]Advanced Water Management Centre, University of Queensland, St. Lucia, QLD 4072, Australia

Edited by Paul G. Falkowski, Rutgers, The State University of New Jersey, New Brunswick, NJ, and approved August 6, 2013 (received for review February 16, 2013)

Increasing atmospheric partial pressure of CO_2 (pCO_2) is a major threat to coral reefs, but some argue that the threat is mitigated by factors such as the variability in the response of coral calcification to acidification, differences in bleaching susceptibility, and the potential for rapid adaptation to anthropogenic warming. However the evidence for these mitigating factors tends to involve experimental studies on corals, as opposed to coral reefs, and rarely includes the influence of multiple variables (e.g., temperature and acidification) within regimes that include diurnal and seasonal variability. Here, we demonstrate that the inclusion of all these factors results in the decalcification of patch-reefs under business-as-usual scenarios and reduced, although positive, calcification under reduced-emission scenarios. Primary productivity was found to remain constant across all scenarios, despite significant bleaching and coral mortality under both future scenarios. Daylight calcification decreased and nocturnal decalcification increased sharply from the preindustrial and control conditions to the future scenarios of low (reduced emissions) and high (business-as-usual) increases in pCO_2. These changes coincided with deeply negative carbonate budgets, a shift toward smaller carbonate sediments, and an increase in the abundance of sediment microbes under the business-as-usual emission scenario. Experimental coral reefs demonstrated highest net calcification rates and lowest rates of coral mortality under preindustrial conditions, suggesting that reef processes may not have been able to keep pace with the relatively minor environmental changes that have occurred during the last century. Taken together, our results have serious implications for the future of coral reefs under business-as-usual environmental changes projected for the coming decades and century.

climate change | carbonate balance | metabolism

Tropical coral reef ecosystems face significant challenges from anthropogenic changes in ocean temperature and chemistry (1). Short periods of anomalously high sea temperatures have triggered mass coral bleaching and mortality events since the early 1980s (2, 3), and projected pH and carbonate ion concentrations reduce the calcification rate of many organisms such as reef-building corals and crustose coralline algae (reviewed in ref. 4). Generally, the projected impacts associated with future increases in sea temperature have been examined independently of those associated with ocean acidification (2, 5–8). When multiple drivers have been considered, extrapolation of the results to the future outlook of coral reefs has been complicated by a lack of replication, the use of artificial light, and/or experimental designs that exclude the potentially important influence of natural variation in ocean temperature and chemistry over diel and seasonal cycles (9–11). Furthermore, most studies have focused on corals or calcareous algae in isolation rather than on broader communities that may better represent the responses of coral reefs (9–11). Excluding the interaction of changing temperature and ocean chemistry, natural variability, and the wider set of organisms and processes places important limitations on our ability to understand the future and ascertain whether, for coral reefs, there is any real difference between action and no action regarding CO_2 emissions. This issue is fundamentally important given the time lag between reducing CO_2 emissions and establishing atmospheric stability, but has not been addressed adequately via studies that seek mechanistic understandings for the individual effects of temperature and acidification on specific organisms, because the sum of the parts may not equal the whole.

Some argue that the potential and imminent threat to coral reefs posed by anthropogenic CO_2 emissions is mitigated by potential rapid evolutionary adaptation by key reef organisms such as corals (12). Within this argument, greater inherent environmental variability is seen as a facilitator of adaptation (13), and the transition within some corals to thermally tolerant symbionts is presented as a current coral plasticity that is likely to enhance adaptation toward warmer water (12). The latter suggestion is debatable because the enhancement in host performance is not typically recorded in terms of a property that belongs uniquely to the host (e.g., coral survival, growth, or reproduction) but rather as properties (bleaching tolerance, sustained maximum quantum yields of photosystem II) that may be more attributable to the symbiont than to the host (14). That is, it is not always clear that the statement "having thermally tolerant symbionts leads to thermally tolerant hosts" is anything more than a tautology. Especially given observations in the current literature that corals harboring thermally tolerant symbionts experience reduced growth (15, 16), that heterotrophic feeding can sustain some coral species postbleaching (17), and finally that while food may be relatively unavailable in the oceans that surround reefs, this is not typically the case on a reef (reviewed in ref. 18). Evolution will occur over multiple generations. Presently, however, we lack the experimental evidence to support scientifically the contention that organism evolution over the next decades will protect features such as the maintenance of a positive carbonate balance that are essential to reef viability and the functional utility of reefs to mankind (1). However, the ocean environment has changed significantly over the last 100 y in terms of both ocean temperature

Significance

The study explores the impact of anthropogenic ocean warming and acidification on intact coral reef assemblages using large-scale, replicated mesocosms that simulate future conditions under natural levels of seasonal variability.

Author contributions: S.G.D., D.I.K., and O.H.-G. designed research; S.G.D. performed research; S.G.D. contributed new reagents/analytic tools; S.G.D., D.I.K., O.P., F.E.A., and G.W.T. analyzed data; and S.G.D., D.I.K., O.P., F.E.A., G.W.T., and O.H.-G. wrote the paper.

The authors declare no conflict of interest.

This article is a PNAS Direct Submission.

Freely available online through the PNAS open access option.

[1]To whom correspondence should be addressed. E-mail: sophie@uq.edu.au.

[2]Present address: Scripps Institute of Oceanography, University of California at San Diego, La Jolla, CA 92093.

This article contains supporting information online at www.pnas.org/lookup/suppl/doi:10.1073/pnas.1302701110/-/DCSupplemental.

Table 1. November composition of the reassembled patch-reefs

Type	Principal components	% cover
Hard coral	*Acropora formosa*; *Seriatopora hystrix**; *Stylophora pistillata*; *Porites cylindrical*; Plating *Montipora* sp.; *Goniastrea aspera*; *Lobophyllia* sp.*; *Fungia* sp.	35 ± 1
Macroalgae	Crustose calcareous algae; red, green, brown filamentous algae; *Halimeda* sp.; *Lobophora* sp.; *Chlorodesmis fastigiata*; *Hypnea* sp.	15 ± 3
Other invertebrates	Zoanthids; *Xenia* sp.; sponges (*Cliona orientalis*); sea cucumbers (*Holothuria atra*); snails (herbivorous); xanthid crabs	2 ± 0
Vertebrates	Three lawnmower blennies (*Salarias fasciatus*)	
Sediments	Skeletons of corals, crustose calcareous algae, foraminifers, mollusks, and Halimeda (39)	48 ± 3

All organisms were collected from a depth of *ca*. 5 m at Harry's Bommie, Heron Island Reef, GBR, Australia.
*Corals excluded from buoyant weight assessment.

and acidification (19, 20), suggesting that reefs in the Southern Great Barrier Reef (GBR), where seasonal environmental variability is great, should provide ample opportunity to evaluate experimentally the degree to which key ecosystem features are retained over decadal time frames.

In the present study, we simulated past and future ocean temperature and chemistry on replicated patches of coral reef reconstructed from a broad range of organisms collected from the growth zone of a coral reef (Harry's Bommie, Heron Island, GBR, 151.9357°E, 23.4675°S) (Table 1 and Fig. S1). The experiment was designed to answer two major questions. The first was whether processes such as the maintenance of maximum net reef calcification rates, measured independently of episodic events such as cyclones, are optimal under the preindustrial (PRE) or present-day (control) scenarios. The second was whether the response of coral reefs differs between action scenarios that result in business-as-usual unabated rates of CO_2 emission (A1FI) as compared to reduced rates of CO_2 emission (B1) through 2050. Here, the Special Report on Emission Scenarios (SRES) A1FI is equivalent to a Representation Concentration Pathway (RCP) 8.5; and, SRES B1 is equivalent to RCP4.5 (21).

To incorporate natural variability at day and seasonal scales, a computer-control system tracked water temperature and ocean partial pressure of CO_2 (pCO_2) look-up tables established from two or three hourly measurements made at our reference site (Harry's Bommie, www.pmel.noaa.gov/co2/story/Heron+Island) during 2010 and 2011 (Fig. S1). Then treatment conditions (with similar natural levels of diurnal and seasonal variability) were established by applying past and projected future anomalies as offsets to these look-up table values (Fig. 1). The precision and accuracy of the control system is evident from the comparison of the data from 2010 and 2011 (black trace in Fig. 1) with the condition replicated in the control (today) mesocosms (blue symbols). PRE conditions were established by reducing the seawater (SW) pCO_2 by 104 ± 11 μatm and temperature by 1 °C. Future conditions were established using anomalies appropriate to the lower (B1: +174 ± 9 μatm, +2 °C) and upper (A1FI: +572 ± 11 μatm, +4 °C) ends of respective scenarios. Temperature profiles for representative mesocosms are shown in Fig. 1, along with the average pH conditions (± SE) measured at 30-min intervals. Experimental treatments were preceded by 2.5 mo in which the coral reef communities were acclimatized to treatment conditions by slowly increasing the relative proportion of treatment water to inner reef flat water [control (field) rates of changes over acclimatization period were 0.04 °C d^{-1} and 6 μatm·pCO_2·d^{-1}; A1FI rates were 0.09 °C·d^{-1} and 14 μatm·pCO_2·d^{-1}]. Full treatments were applied over the austral summer from early November 2011 to early February 2012 under light conditions appropriate to the reference site.

Results and Discussion

Different treatments had different impacts on community composition as well as on the incidence of coral bleaching and mortality (Wilks' multivariate test, $F_{(18,\ 8.97)} = 5.01$, $P < 0.0091$). Weekly images taken of each mesocosm [Fig. 2, Figs. S2 and S3, and Movies S1 (PRE), S2 (control), S3 (B1), and S4 (A1FI)] revealed the large differences in coral bleaching and mortality among treatments. Although most corals had begun to pale in the A1FI scenario by the beginning of November, the control and B1 mesocosms manifested large amounts of bleaching only in the early part of February. Bleaching was seen in the PRE treatment only in the coral *Seriatopora hystrix*, which is temperature sensitive (22). Likewise, the level of bleaching observed under control conditions was consistent with Heron Island's being placed under a Bleaching Watch (the lowest warning level) in January and February 2011 by the Coral Reef Watch program at the National Oceanic and Atmospheric Administration (http://coralreefwatch.noaa.gov). Although many coral species survived these mild levels of thermal stress, colonies growing in the upper and lower future scenarios experienced significant mortality [$F_{(3,8)} = 155.61$, $P < 0.0001$; post hoc: PRE = C < B1 = A1FI]

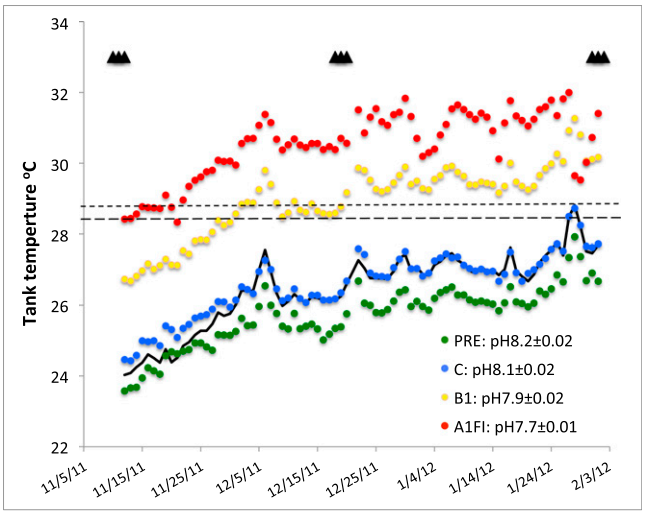

Fig. 1. Treatment conditions established over the experimental period: daily temperature profiles and average treatment pH obtained through the course of the experiment. PRE, pre-industrial treatment; C, control treatment set to mimic conditions at the reference site (Harry's Bommie, GBR, Australia, indicated by the solid black line) measured by the Commonwealth Scientific and Industrial Research Organization between November 2010 and February 2011; B1, SRES B1/RCP4.5, reduced CO_2 emission scenario; A1FI, SRES A1FI/RCP 8.5 business-as-usual emissions scenario. The upper dashed line represents the maximum monthly mean (MMM) + 1 °C, established for Heron Island using 50-km pixel satellite data (http://coralreefwatch.noaa.gov). The lower dashed line represents MMM+1 specific to the reference site established by relating satellite nighttime temperatures to same-day average night temperatures logged at Harry's Bommie. Triangles represent sampling days for community O_2 flux and calcification measurements. Average pCO_2s across sampling days were PRE = 301 ± 11 μatm, C = 405 ± 25 μatm, B1 = 611 ± 17 μatm, and A1FI = 1,009 ± 8 μatm (Table S1).

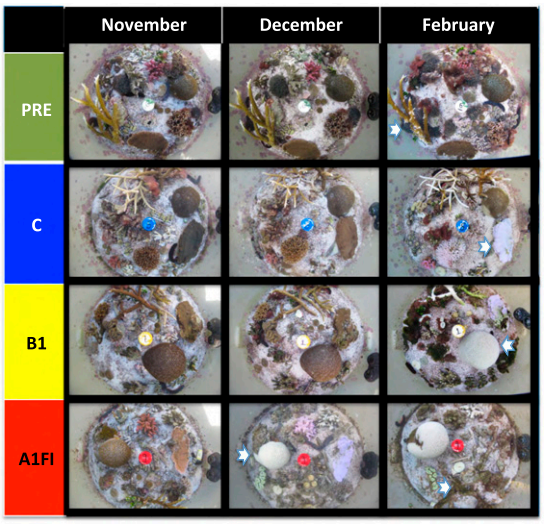

Fig. 2. Photographs of patch-reefs from different treatments through time (set 1 of 3; for sets 2 and 3, see Figs. S2 and S3, respectively). Photographs were taken in the late afternoon with a PowerShot G12 camera (Canon) and are representative of the status of the experimental patch-reefs at the O_2 flux and calcification sampling points in November, December, and February. Arrows highlight growth of new apical branches on *Acropora formosa* (PRE, February), bleached *Montipora* plate (C, February), bleached *Goniastrea* (B1, February, and A1FI, December). The complete series of photographs is available (Movies S1–S4).

(Fig. 3*A*). In this case, *Acropora*, *Seriatopora*, *Montipora*, and *Stylophora* colonies died and were overgrown by algae; colonies of *Goniastrea*, *Lobophyllia*, and *Fungia*, survived to the end of the experiment without shrinkage or overgrowth, although they exhibited severe bleaching for more than 2 mo. *Porites* also survived in a bleached state, although it remained able to remove biofilms by periodic sloughing of the surface mucus layer (Movie S4, A1FI). The observation that bleached corals can survive for a prolonged period over the summer months shows that many hard corals common to the GBR are not overly dependent on their symbionts for energy acquisition (17, 18).

Our understanding of how community processes are likely to change under rapid anthropogenic climate change is poor. In the present experiment, rates of net community primary (1°) productivity and calcification were determined by measuring the responses of the 12 replicated patch-reefs (Fig. S1). Table S1 provides seawater parameters over sampling days, and Fig. S4 provides averaged data at four time points within 24-h periods). Net community 1° productivity varied with summer month, being highest in December over the summer solstice (equivalent to 3.8 g $C{\cdot}m^{-2}{\cdot}d^{-1}$, applying a conversion coefficient of 0.375, the molar ratio of C to O_2) and lowest in November (>1.5 g $C{\cdot}m^{-2}{\cdot}d^{-1}$; $F_{(2,16)} = 27.6$; post hoc, December > February > November) (Fig. 3 *B* and *C*). Rates of net 1° productivity were indistinguishable across the four experimental treatments, a result that is similar to previous studies with respect to both differential community composition (−1.0 to 5.1 g $C{\cdot}m^{-2}{\cdot}d^{-1}$) (23) and differential levels of acidification (equivalent to 1.5 g $C{\cdot}m^{-2}{\cdot}d^{-1}$) (7). However, the rates of net summer reef calcification showed strong treatment effects [$F_{(3,8)} = 40.11$, $P < 0.00004$] (Fig. 3*D*).

Patch-reef calcification rates under the A1FI business-as-usual scenario were consistently negative and were significantly different from the reduced (although still positive) net rates of calcification obtained under the B1 scenario (post hoc: PRE > control > B1 > 0 > A1FI patch-reef calcification rates). Investigating variation in this parameter over the diel cycle revealed high levels of nighttime carbonate dissolution (maximum: 0.23 g $CaCO_3{\cdot}h^{-1}$), mostly under A1FI conditions (Fig. S4) but becoming more evident with the progression of summer under control and B1 scenarios, matching the general decrease in daytime calcification over time in scenarios representing increasing concentrations of atmospheric pCO_2 (November to February) (Fig. 3*E*). Rates of coral calcification were followed using changes in the buoyant weight (24) for six species of corals established in the reef communities (Table 1). The rate of colony calcification, relative to initial buoyant weight, was highest in corals growing in the PRE treatment, with control corals subsequently having significantly higher calcification rates than corals from both future scenarios, which had calcification rates that were indistinguishable from zero [$F_{(3,63)} = 5.82$), $P < 0.0015$; post hoc: PRE = control > B1 = A1FI] (Fig. 3*F*). However, measurement of sediment grain size revealed that the sediments in A1FI conditions had a significantly greater percentage of small grains (less than 0.5 mm) than all other treatments [$F_{(3,8)} = 6.19$, $P < 0.018$; post hoc, $P < 0.05$] (Fig. 3*G*).

The most likely explanation for our results is that greater nocturnal decalcification under the business-as-usual scenario reduced carbonate resources principally associated with the sediments, with bioerosion of dead coral branches potentially also contributing to the effect (25). Diel variations in the rates of sediment decalcification have been observed previously for coral reef locations where nocturnal sediment dissolution was found to be associated with increased concentrations of CO_2 associated with high rates of aerobic respiration (26). Likewise, net increases in sediment dissolution have been observed for field sites and experimental mesocosms where the overlaying seawater is naturally or artificially acidified (27). Sediment dissolution frequently is identified with either the decalcification of the more soluble high-Mg calcite components under elevated pCO_2 and/or with the metabolic stimulus of microbial aerobic respiration within the pore waters immediately adjacent to the sediments (27). In our experiment, the total community respiration rates of the experimental reefs were unaffected by changes in community structure (Fig. 3). This observation, however, does not preclude the possibility that a relatively isolated compartment of the ecosystem may experience altered respiration under different scenarios. The sediment-associated microbial communities were dominated by ammonium-oxidizing bacteria and archaea, photosynthetic bacteria, and aerobic heterotrophs (Fig. 4). The scenarios did not differ significantly in the relative abundance of various bacterial and archaeal genera (Fig. 4 and Fig. S5). However, the total microbial biomass was significantly higher in the business-as-usual scenario than in other scenarios (Fig. 4 and Fig. S6). Although we did not measure microbial metabolism explicitly, it is possible that increases in microbial biomass, supported by high temperature, were linked to increases in the nighttime production of CO_2 and hence to sediment decalcification. Alternatively, a constant (*ca.* 0.6) nighttime decrease in pH between layering seawater and sediment pore-water (28) may account for the differential decalcification rates observed among scenarios, with the smaller sediments in the business-as-usual scenario providing a greater surface area to harbor microbes. Notably, anaerobic sulfate- or nitrate-reducing microorganisms were absent from all scenarios, including the business-as-usual scenario, suggesting that increases in nocturnal alkalinity were not driven by these particular microbial processes but rather by patch-reef decalcification (27).

Our results show that the current business-as-usual pathway is very likely to have serious impacts on coral reef ecosystems over summer periods when temperatures and seawater pCO_2 concentrations are at their highest (www.pmel.noaa.gov/co2/story/Heron+Island). Under this scenario, carbonate substrates will tend to dissolve, and the community structure will bear little resemblance to the coral-dominated reefs of today. It is unlikely that winter periods will offer sufficient time for recovery from the observed devastation, because such recovery typically takes years, not months (3). The unlikeliness of recovery is supported further by data regarding coral $CaCO_3$ accretion under the net annual or winter A1FI scenario (Fig. S7). Collectively, the data suggest further depletions, rather than recovery, in reef $CaCO_3$

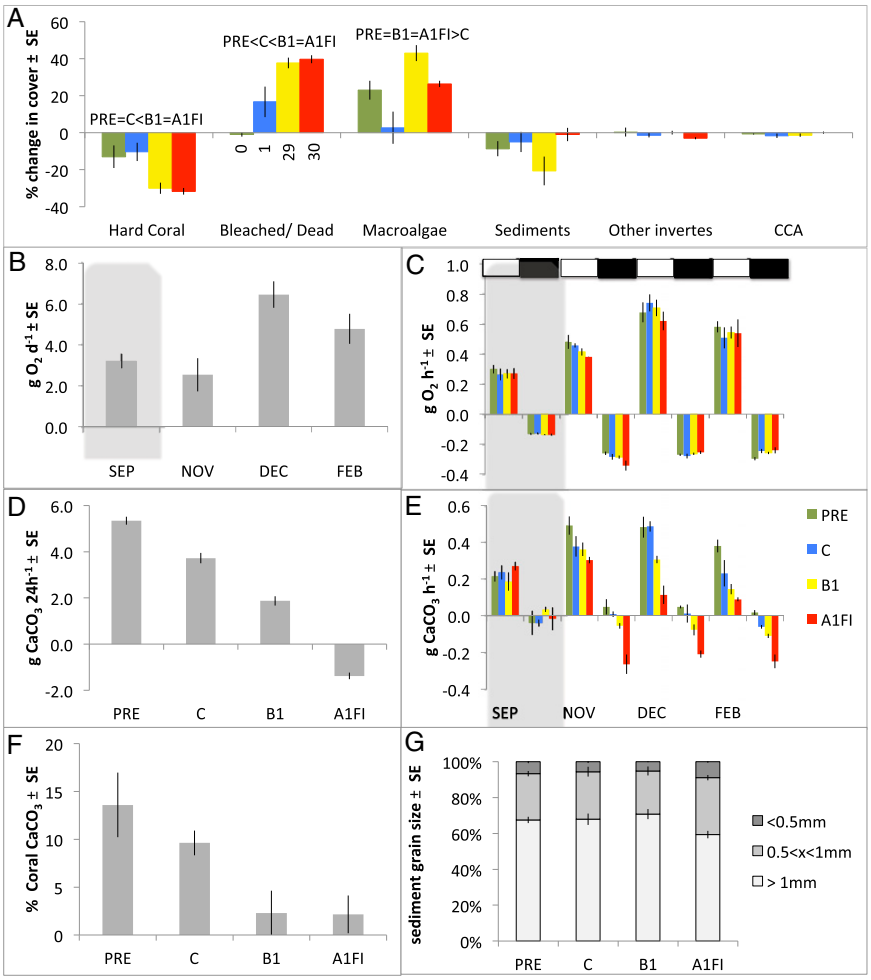

Fig. 3. Responses of experimental reefs to seawater conditions associated with differing levels of atmospheric CO_2 in the experimental scenarios. (*A*) Changes in the percent cover for different reef components between November, when treatment conditions were first attained, and early February, when the experiment was terminated. Hard Coral, reef-building coral with natural complements of symbiotic dinoflagellates; Bleached/Dead, bleached or dead and algal-covered reef-building corals (the percentage of change in dead-only coral cover is shown by the numerals immediately below the *x*-axis); Macroalgae includes algae covering dead coral; Other invertes, other invertebrates; CCA, crustose calcareous algae. Post hoc differences are provided above the relevant data. (*B*) Mean monthly O_2 flux projected over a 24-h period from measurements taken at midday, after sunset, at midnight, and after sunrise. September (SEP) data are shaded because they represent the pretreatment condition. (*C*) Day (under white bars) vs. night (under dark bars) O_2 flux through time and across treatment. September (SEP) data are shaded because they represent the pretreatment condition. (*D*) Net daily summer calcification rates estimated by averaging November, December, and February responses. (*E*) Midday (under white bars) vs. midnight (under dark bars) calcification rates through time and across treatment. September (SEP) data are shaded because they represent the pretreatment condition. (*F*) Percentage of change in coral buoyant weight between November and February relative to initial buoyant weight. (*G*) Grain size distribution among treatments measured in February.

under a winter A1FI scenario, especially following large-scale coral mortality (Fig. S7). Our results also demonstrate that strongly reducing CO_2 emissions is likely to result in the more optimistic outcome of reduced but nonetheless positive rates of net reef calcification. Dissolution of sediments is unlikely to have an impact on aragonite or calcite saturation states in surrounding waters given that coral reefs, like the experimental system used here, are well flushed by the open ocean (29). However, reductions in sediment grain size are likely to have an impact on lateral reef growth and consolidation (30, 31) and on the formation of coral cays (32). Perhaps of great interest is the observation that PRE conditions resulted in higher reef and coral calcification rates and reduced levels of coral mortality and bleaching, matching field observations (33) and suggesting that, despite the passage of more than 100 y, the key Heron Island reef assemblages included in the present study are better suited to conditions that occurred in the past than to those of the present day. This outcome is entirely consistent with the attribution of cyclones as major drivers for recent GBR decline (34), because reductions in reef net calcification will lead to slower recovery from these episodic events. This final result has important implications for current speculations as to whether coral reef ecosystems will be able to adjust over the next 100 y to preserve the array of key ecological goods and services that typically are associated with their $CaCO_3$ structures.

Materials and Methods

Organisms were collected under Great Barrier Reef Marine Park permit number G11/34172.1.

Seawater was drawn continuously from the inner coral reef flat of Heron Island and was manipulated within four 8,000-L sumps with CO_2 and temperature control and then was fed into 12 (three per treatment) 300-L mesocosms in which representative coral reef communities had been established (Fig. 1*A*). Natural irradiance was provided by filters (Marine Blue #131; Lee Filters) and corresponded to summer light spectra and intensities measured at the reference site (150 μmol·quanta·m^{-2}·s^{-1} averaged over 24 h). As described in the text, four distinct scenarios were established representing preindustrial, present (control), and future ocean conditions for the upper reef slope environment of the reference site (Fig. S1).

Patch-Reef Reconstruction. The patch-reefs used in the present study were collected using SCUBA over a period of 4 mo from a depth of *ca*. 5 m at the reference sites. Sediments were maintained in seawater at all times, mixed, and randomly allocated to form a base with a depth of 2.5 cm in each mesocosm. Then equal volumes of live rock were introduced into the tanks. The live rock was used to support corals above the sediments. Live rock also was used to wedge the branching corals in an upright position. The calcareous green alga, *Halimeda sp.*, was placed under the *Acropora* branches, as at the reference site. Hard corals (together with infauna) were collected using a hammer and chisel. Algae and soft corals were collected together with adhering coral rubble to prevent damage to thalli or stems. Blennies were collected using clove oil and a hand net. All other organisms were collected by hand. All organisms (Table 1) were transported in water and under shade cloth from the field site to the research station, where they were distributed directly and equally among the mesocosm tanks. This distribution resulted in 12 nearly identical patch-reefs that represented the diversity of organisms found at the reference sites with gaps left between organisms to allow for growth. Organisms that failed to survive were replaced, and the pretreatment acclimatization period was delayed until all patch-reefs were equally well established.

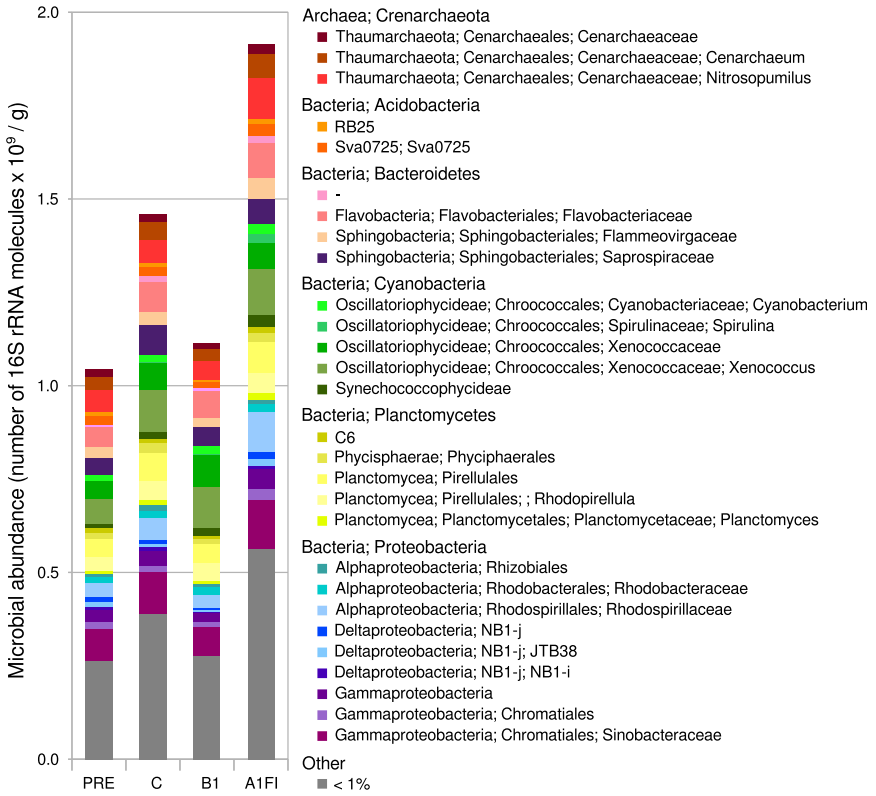

Fig. 4. Composition and abundance of bacterial and archaeal genera associated with the sediments under different scenarios. Sediment samples collected in February from each scenario (a total of five samples for each scenario: three samples from a single tank under each scenario and one additional sample from the two other replicate tanks for the scenario) were analyzed using *16S rRNA* gene amplicon sequencing and qPCR. The total microbial biomass was estimated from the number of *16S rRNA* gene molecules per gram of sediments, and *16S rRNA* gene amplicon sequencing was used to determine the taxonomic composition of each community. Each bar represents the average community composition of the samples from each scenario, weighted by the average estimated biomass. Other, genera present at a relative abundance of less than 1% in all scenarios.

pCO_2/Temperature System. The pCO_2/temperature (pCO_2/T) system manipulates seawater pCO_2 and temperature levels using feedback control systems. The pCO_2 control system used one central pCO_2 sensor (CO_2-PRO; Pro-Oceanus Systems) that received seawater from the four experimental sumps. The pCO_2 levels were logged by a central computer system and used to control (using custom-made software; SCIWARE Software Solutions) the injection of CO_2 enriched to 30% or CO_2-free air to regulate the pCO_2 concentrations in each of the experimental pCO_2/T treatments as required by the look-up table established from the reference site. The appropriate mix of 30% CO_2 or CO_2-free air was delivered to the 8,000-L sump via a fine curtain of bubbles. CO_2 was mixed to 30% CO_2 using an inline gas mixer (Mg100-2ME; Witt) fed by bottled CO_2 (BOC Australia) and compressed air (Airmac T55 415V). CO_2-free air was produced by passing compressed air through two desiccant columns (Model 106-C; W. A. HAMMOND DRIERITE) filled with Spherasorb Soda Lime (Mayo Healthcare). The temperature in each sump was controlled by a heater-chiller (HWPO17-1BB; Rheem) responding to mesocosm tank temperatures (PT100 thermocouples; RS Components) and set to follow a look-up table established from the reference site with the assistance of a custom-made software program. The 8,000-L sumps (2.23 m × 2.23 m × 1.63 m) were constructed from fiberglass around a stainless steel frame with lids also made from fiberglass. The sumps were filled continuously by water pumped from the inner reef flat of Heron Island (GBR, Australia) and filtered through a sand filter (CCF21-0; Davey) to remove large sediment particles that have the potential to lodge in the pCO_2 sensor but to allow the passage of particles smaller than 10 μm. Then seawater from each of the four sumps was pumped into three mesocosm tanks per scenario at a flow rate of 4.3 $L{\cdot}min^{-1}$. Circulation within each mesocosm tank was enhanced by the action of a dual-blower wave-maker (JVP 12000L/H; ProAqua). pH (National Institute of Standards and Technology scale) in these mesocosm tanks was measured by pH sensors (InPro4501VP; Mettler Toledo) connected to a monitoring system (ACQ110; Aquatronica); however, these pH readings were for information only and were not used to control CO_2 dosing.

Composition Analysis. Changes to the percentage of cover by the different reef components between November, when treatment conditions were first attained after an acclimatization period of 2.5 mo, and early February, when the experiment was terminated, were estimated from photographs ($n = 3$ per treatment at each time point) annotated with 100 random points using CoralNet (http://coralnet.ucsd.edu).

Measurements of 1° Productivity and Calcification Rate. Mesocosm tanks were constructed so that lids covered with Marine Blue filter paper (#131; Lee Filters) could be inserted into the tanks to provide an airtight seal on the surface of the water. Before introducing treatment conditions (in early September), as treatment conditions were attained (in November), at mid treatment (in December), and at the termination of treatment (in February), the mesocosm tanks were sealed, the water input was turned off, with the dual-blower wave-maker left on to ensure flow within the tanks, between 12–13 h, 18–20 h, 0–2 h, and 7–9 h. Before sealing tanks, an O_2 sensor (RINKO ARO-USB; JFE Advantech) was introduced and set to log O_2 concentrations at 1-min intervals. Water samples (100 mL) were taken for alkalinity measurements immediately after each tank was sealed and just before the tank was unsealed 1–2 h later. The time between samples was recorded. The alkalinity of seawater samples was analyzed by titration (T50 titrator; Mettler Toledo) and was calibrated with a Dickson standard as described by Kline et al. (35). Under aerobic conditions and constant salinity, net $CaCO_3$ dissolution or precipitation is determined from observed changes in seawater alkalinity. (36).

Analysis of Sediment Grain Size. Sediments were collected from the tanks at the termination of the experiment. Sediment samples (1 L) were dried overnight at 60 °C before being passed through a sieve shaker (Minor M200; Endecotts). Sieved fractions were weighed to determine the percentage (wt/wt) of each size class present in each sample.

Analysis of Sediment-Associated Microbial Community. Sediment microbes were sampled in February when the experiment was terminated. Sediments were collected directly into sterile 5-mL tubes from the surface layer (1–2 cm) of the sediments, and excess water was poured off before the sediments were flash-frozen in liquid N_2 and stored at −80 °C. Total genomic DNA extraction was carried out using the PowerBiofilm DNA Isolation Kit (MoBio Laboratories Ltd.); 250 mg of well-mixed thawed sediments were extracted following the manufacturer's instructions. Universal primers with the 454 pyrotag adapter ligated at the 5′ end (pyroLSSU926F 5′-AAACTYAAAK-GAATTGRCGG-3′ and pyroLSSU1392R 5′-ACGGGCGGTGWGTRC-3′) were used to amplify a region of the *16S rRNA* gene (see *SI Text*). Amplicon size section was carried out using the Pippin Prep System (Sage Science) before sequencing on a 454 Life Science Genome Sequencer GS FLX Ti (Roche) at the Australian Centre for Ecogenomics, The University of Queensland.

Amplicon reads were processed through a modified QIIME pipeline (37). Amplicon reads were first passed through Acacia (38) for correction of 454 homopolymer errors and trimming. Chimeric reads were deleted using UCHIIME. UCLUST was run to form operational taxonomic units (OTUs) at 97% sequence identity. To make taxonomic assignments, the OTU representative sequences were compared with a custom database (all bacteria and archaea from the Greengenes database (http://greengenes.lbl.gov/) and the eukarya from the Silva database, http://www.arb-silva.de/) using BLASTN. An OTU table was constructed from these results, and OTUs represented by a single sequence were excluded. All reads matching eukaryotes or chloroplasts were removed before rarefaction to 400 reads (using 1,000 bootstrap repetitions). Taxonomic assignments were summarized at the genus level.

A quantitative PCR (qPCR) analysis was performed to quantify microbial abundance (see *SI Text*). The primers, 1406F (5′-GYACWCACCGCCCGT-3′) and 1525R (5′-AAGGAGGTGWTCCARCC-3′), were used to amplify all bacterial and archaeal *16S rRNA* genes. Tenfold dilutions of *Escherichia coli* DNA from 800–0.08 pg were used to produce a standard curve. Inhibition controls included amplification with primers (0.2 μM) designed to target the *E. coli* rpsL gene (forward primer: 5′-GTAAAGTATGCCGTGTTCGT-3′, and reverse primer: 5′-AGCCTGCTTACGGTCTTTA-3′). Two dilutions, 1/500 and 1/1,000 (microbial template DNA; 1406F/1525R primer set), as well as an inhibition control (*E. coli* DH10B genomic DNA; rpsL primer set) were run in triplicate for each sample. The cycle threshold values were recorded and compared with the standard curve using ABI SDS 2.4.1 software.

Statistical Analysis. O_2 flux and calcification rate data were analyzed using two-factorial repeated-measures ANOVA. The within-subject factor was Month determined at three experimental time points: beginning (November), mid (December), and end (February). The categorical factor was Treatment analyzed at four different levels (PRE, control, B1, and A1FI) with three replicate mesocosms per level.

Changes in the reef-community compositions were analyzed by Wilks' lambda multivariate testing of significance using as variables the components identified in Fig. 3*A*. Components were subsequently analyzed by one-factorial ANOVAs with the categorical factor Treatment. Likewise, changes to coral buoyant weight relative to initial weight and differences in sediment grain size were analyzed by one-factorial ANOVAs with the categorical factor Treatment. Assumptions of homogeneity were tested using Cockran's C test, and post hoc analysis was performed by the Newman–Keul method.

Changes in the microbial-community composition was determined by calculating the generalized UniFrac distance (d = 0.5) between microbial profiles (GUniFrac function of the GUniFrac package in R, version 2.15.1) using a PERMANOVA test, with treatments as grouping factors (adonis function of the vegan package in R version 2.15.1, http://www.R-project.org/). Differences in total microbial abundance, based on qPCR, were established using a single-sided Mann–Whitney test between each pair of treatments (wilcox.test function in R version 2.15.1).

ACKNOWLEDGMENTS. We thank Dr. Bronte Tillbrook, Annamieke Van Den Heuvel, Aaron Chai, Giovanni Bernal Carrillo, Emmanuelle Zoccola, Dr. Pim Bongaerts, Dorothea Bender, James Fang, Catalina Reyes Nivia, Novi Adi, Matheus Athayde, Dr. Fiona May, Nancy Lachner, Mirta Zupan, Zoe Reynolds, and Chantelle Reid for their assistance. The experiment was co-funded by the Great Barrier Reef Foundation, the Australian Research Council (ARC) Centre for Excellence in Coral Reef Studies (CE0561435), ARC Linkage (LP0775303), and a Queensland Smart State Fellowship (to O.H.-G.).

1. Hoegh-Guldberg O, et al. (2007) Coral reefs under rapid climate change and ocean acidification. *Science* 318(5857):1737–1742.
2. Hoegh-Guldberg O (1999) Coral bleaching, climate change and the future of the world's coral reefs. *Mar Freshw Res* 50(8):839–866.
3. Baker A, Glynn PW, Riegl B (2008) Climate change and coral reef bleaching: An ecological assessment of long-term impacts, recovery trends and future outlook. *Estuar Coast Shelf Sci* 80(4):435–471.
4. Doney SC, Fabry VJ, Feely RA, Kleypas JA (2009) Ocean acidification: The other CO_2 problem. *Annu Rev Mar Sci* 1:169–192.
5. Kleypas JA, et al. (1999) Geochemical consequences of increased atmospheric carbon dioxide on coral reefs. *Science* 284(5411):118–120.
6. Langdon C, et al. (2003) Effect of elevated CO_2 on the community metabolism of an experimental coral reef. *Global Biogeochem Cycles* 17(1):1–14.
7. Leclercq N, Gattuso J, Jaubert J (2002) Primary production, respiration, and calcification of a coral reef mesocosm under increased CO_2 partial pressure. *Limnol Oceanogr* 47(2):558–564.
8. Kuffner LB, Andersson AJ, Jokiel PL, Rodgers KS, Mackenzie FT (2008) Decreased abundance of crustose coralline algae due to ocean acidification. *Nat Geosci* 1:114–117.
9. Reynaud S, et al. (2003) Interacting effects of CO_2 partial pressure and temperature on photosynthesis and calcification in a scleractinian coral. *Glob Change Biol* 9(11):1660–1668.
10. Anthony KR, Kline DI, Diaz-Pulido G, Dove S, Hoegh-Guldberg O (2008) Ocean acidification causes bleaching and productivity loss in coral reef builders. *Proc Natl Acad Sci USA* 105(45):17442–17446.
11. Langdon C, Atkinson M (2005) Effect of elevated pCO_2 on photosynthesis and calcification of corals and interactions with seasonal change in temperature/irradiance and nutrient enrichment. *J Geophys Res* 110(C9):C09S07.
12. Pandolfi JM, Connolly SR, Marshall DJ, Cohen AL (2011) Projecting coral reef futures under global warming and ocean acidification. *Science* 333(6041):418–422.
13. Berkelmans R, Willis BL (1999) Seasonal and local spatial patterns in the upper thermal limits of corals on the inshore Central Great Barrier Reef. *Coral Reefs* 18(3):219–228.
14. Berkelmans R, van Oppen MJ (2006) The role of zooxanthellae in the thermal tolerance of corals: A 'nugget of hope' for coral reefs in an era of climate change. *Proc Biol Sci* 273(1599):2305–2312.
15. Little AF, van Oppen MJ, Willis BL (2004) Flexibility in algal endosymbioses shapes growth in reef corals. *Science* 304(5676):1492–1494.
16. Jones A, Berkelmans R (2010) Potential costs of acclimatization to a warmer climate: Growth of a reef coral with heat tolerant vs. sensitive symbiont types. *PLoS ONE* 5(5):e10437.
17. Grottoli AG, Rodrigues LJ, Palardy JE (2006) Heterotrophic plasticity and resilience in bleached corals. *Nature* 440(7088):1186–1189.
18. Houlbrèque F, Ferrier-Pagès C (2009) Heterotrophy in tropical scleractinian corals. *Biol Rev Camb Philos Soc* 84(1):1–17.
19. Feely R, Doney S, Cooley S (2009) Ocean acidification: Present conditions and future changes in a high-CO_2 world. *Oceanogr* 22(4):36–47.
20. Roemmich D, John Gould W, Gilson J (2012) 135 years of global ocean warming between the Challenger expedition and the Argo Programme. *Nat Climate Change* 2(6):425–428.
21. Rogelj J, Meinshausen M, Knutti R (2012) Global warming under old and new scenarios using IPCC climate sensitivity range estimates. *Nat Climate Change* 2(4):248–253.
22. Marshall P, Baird A (2000) Bleaching of corals on the Great Barrier Reef: Differential susceptibilities among taxa. *Coral Reefs* 19(2):155–163.
23. Hatcher BG (1990) Coral reef primary productivity. A hierarchy of pattern and process. *Trends Ecol Evol* 5(5):149–155.
24. Spencer Davies P (1989) Short-term growth measurements of corals using an accurate buoyant weighing technique. *Mar Biol* 101(3):389–395.
25. Reyes-Nivia C, Diaz-Pulido G, Kline D, Guldberg OH, Dove S (2013) Ocean acidification and warming scenarios increase microbioerosion of coral skeletons. *Glob Change Biol* 19(6):1919–1929.
26. Yates KK, Halley RB (2006) Diurnal variation in rates of calcification and carbonate sediment dissolution in Florida Bay. *Est Coasts* 29(1):24–39.
27. Andersson AJ, Bates NR, Mackenzie FT (2007) Dissolution of carbonate sediments under rising pCO_2 and ocean acidification: Observations from Devil's Hole, Bermuda. *Aquat Geochem* 13(3):237–264.
28. Stahl H, et al. (2006) Time-resolved pH imaging in marine sediments with a luminescent planar optode. *Limnol Oceanogr Methods* 4:336–345.
29. Andersson AJ, Mackenzie FT, Ver LM (2003) Solution of shallow-water carbonates: An insignificant buffer against rising atmospheric CO_2. *Geology* 31(6):513–516.
30. Kennedy D, Woodroffe C (2002) Fringing reef growth and morphology: A review. *Earth Sci Rev* 57(3-4):255–277.
31. Hughes T (1999) Off-reef transport of coral fragments at Lizard Island, Australia. *Mar Geol* 157(1):1–6.
32. Woodroffe CD, Samosorn B, Hua Q, Hart DE (2007) Incremental accretion of a sandy reef island over the past 3000 years indicated by component-specific radiocarbon dating. *Geophys Res Lett* 34(L03602):1–5.
33. De'ath G, Lough JM, Fabricius KE (2009) Declining coral calcification on the Great Barrier Reef. *Science* 323(5910):116–119.
34. De'ath G, Fabricius KE, Sweatman H, Puotinen M (2012) The 27-year decline of coral cover on the Great Barrier Reef and its causes. *Proc Natl Acad Sci USA* 109(44):17995–17999.
35. Kline DI, et al. (2012) A short-term in situ CO_2 enrichment experiment on Heron Island (GBR). *Sci Rep* 2:413.
36. Chisholm JRM, Gattuso JP (1991) Validation of the alkalinity anomaly technique for investigating calcification and photosynthesis in coral reef communities. *Limnol Oceanogr* 36(6):1232–1239.
37. Caporaso JG, et al. (2010) QIIME allows analysis of high-throughput community sequencing data. *Nat Methods* 7(5):335–336.
38. Bragg L, Stone G, Imelfort M, Hugenholtz P, Tyson GW (2012) Fast, accurate error-correction of amplicon pyrosequences using Acacia. *Nat Methods* 9(5):425–426.
39. Maxwell W, Jell J, McKellar R (1964) Differentiation of carbonate sediments in the Heron Island reef. *J Sediment Res* 34(2):294–308.